

T. KAWABATA*, T. NAMIKI*, K. MATSUDA*, D. TOKAI*, S. MURAKAMI*, K. NISHIMURA*

SUPERCONDUCTIVITY OF MgB₂ COMPOSITED WITH Mg-Zn ALLOYS

NADPRZEWODNICTWO KOMPOZYTÓW MgB₂ – STOP Mg-Zn

The three-dimensional penetration method combined with semi-solid casting was used to fabricate metal-powder composite superconducting materials of MgB₂ with magnesium alloys: MgB₂/Mg - *x*wt% Zn (*x* = 1, 3, 6, 9). X-ray diffraction measurements indicated predominant peak patterns of MgB₂ and a host alloy. Measured electrical resistivity (ρ) versus temperature showed a clear signal of superconducting transition at about 34 K for all the samples cut out from the composites. External field (*H*) dependence of $\rho(T, H)$ provided upper critical field of about 5 T. A volume fraction of the superconducting state of the sample estimated from a low external field part of magnetization was almost the same as the nominal ratio of MgB₂ powder against the host material. A magnetic hysteresis loop observed at 5 K suggested that an addition of Zn element to magnesium host-matrix little changed the critical current density (J_c). A comparison of the present results with the previous ones of MgB₂/Mg-Al-Zn systems confirmed that simultaneously doped Al and Zn were necessary to enhance J_c . Specific heat measurements of the sample with an external field showed that the bulk superconductivity of MgB₂ was well conserved in the composites.

Keywords: MgB₂, composite materials, magnesium alloy, specific heat

Metodę trójwymiarowego zagęszczania w połączeniu z odlewaniem w stanie stało-ciekłym użyto do wytworzenia kompozytowych materiałów nadprzewodzących proszku MgB₂ ze stopami magnezu MgB₂/Mg - *x* % wag Zn (*x* = 1, 3, 6, 9). Rentgenowskie pomiary dyfrakcyjne wykazały obecność wyraźnych pików od MgB₂ i osnowy. Oporność elektryczna (ρ) mierzona w zależności od temperatury zawierała wyraźny sygnał przejścia nadprzewodzącego około 34 K dla wszystkich próbek wyciętych z kompozytów. Zależność $\rho(T, H)$ od zewnętrznego pola (*H*) pokazała górną krytyczną wartość pola 5 T. Udział objętościowy próbki w stanie nadprzewodzącym oszacowany z niskiej części zewnętrznego pola magnetyzacji był prawie taki sam jak stosunek nominalnej zawartości proszku MgB₂ do materiału osnowy. Pętla histerezy magnetycznej obserwowana przy 5 K sugeruje, że dodatek Zn do osnowy magnezowej niewiele zmienia gęstość prądu krytycznego (J_c). Porównanie obecnych wyników z wcześniej uzyskanymi dla układów MgB₂/Mg-Al-Zn potwierdziło, że do zwiększenia J_c konieczne jest jednoczesne domieszkowanie Al i Zn. Pomiary ciepła właściwego próbki w zewnętrznym polu wykazały, że nadprzewodnictwo MgB₂ zostało dobrze zachowane w kompozytach.

1. Introduction

Attractive points of superconducting properties of MgB₂ are high critical temperature (T_c) [1] among metallic compounds, relatively large upper critical field [2], isotropic transport properties against the crystallographic directions [3], and rather long coherence length [4], which stimulate plenty of research activities to develop suitable processes for producing MgB₂ wires and tapes [5, 6]. For practical use, the critical current density (J_c) of MgB₂ has been one of major issues of research; a well known problem is that J_c drops rapidly with increasing magnetic field due to its poor flux pinning. Improvements in J_c (enhancements of flux pinning) were achieved by various approaches; doping by chemical compounds [7], substitution of Mg and/or B by other elements [8, 9], high-pressure application during process [10], various heat-treatment [11], etc. Theoretical studies for variations of

the band structure by element substitution were also carried out [12-14]. The consistent interpretation for J_c variations with fabrication processes has been given via the comprehensive studies of normal-state resistivity of MgB₂ by Yamamoto et al [15-17], using MgB₂ bulk samples with systematically varied packing factors (density).

The three-dimensional penetration method combined with semi-solid casting (SS-3DPC) has been successfully used to fabricate metal-powder composite superconducting materials [18]. This is a kind of the ex-situ technique, in which a half-melted host metal, such aluminum or magnesium, penetrated MgB₂ powder-preform by pressure. A low temperature casting is a great advantage of SS-3DPC compared the powder-in-tube (PIT) method [19], in which high temperature heat treatments easily introduced large voids in MgB₂ grains. Our previous work on MgB₂/Al composite materials demonstrated that the superconducting transition tempera-

* GRADUATE SCHOOL OF SCIENCE AND ENGINEERING, UNIVERSITY OF TOYAMA, 3190, GOFUKU, TOYAMA, 930-8555, JAPAN

ture (T_c) was observed at 38 K on the resistivity, a superconducting volume fraction estimated from magnetization was about 50% [18], and further a superconducting wire of MgB_2/Al of 1mm diameter was extruded [20]. Experimental results of MgB_2 -powder composite materials with the magnesium-aluminum-zinc alloys prepared by the SS-3DPC technique have been given elsewhere [21], which elucidated that doping Al and Zn elements enhanced J_c . This result facilitates a study of the $\text{MgB}_2/\text{Mg-Zn}$ system to investigate if the enhancement of J_c originated in doped Zn, since Zn has been known to increase T_c of MgB_2 [22]. This paper deals with the MgB_2 composited samples with host materials of Mg-x wt\% Zn ($x = 1, 3, 6, 9$, hereafter noted as Z1, Z3, Z6, Z9, respectively). The results are compared with our previous ones of MgB_2/Mg (noted as M0) and $\text{MgB}_2/\text{Mg-9wt\%Al-1\%Zn}$ (AZ91) samples [21].

2. Experimental

MgB_2 powders provided from Kojundo Chemical Laboratory have a purity of more than 99%, and an averaged grain-size was approximately $40 \mu\text{m}$. The details of sample preparation have been given elsewhere [18, 21]. A conventional scanning electron microscope (SEM) was used to inspect the MgB_2 powders and host materials in the composites. Figure 1 illustrates a typical SEM image at a cut surface of the obtained billet of $\text{MgB}_2/\text{Mg-9wt\%Zn}$. It is clear that the magnesium host metal (gray-white area) tightly bound MgB_2 particles (dark-gray shape). A density of the central part of the billet was about 2.1 g/cm^3 , which is in between those of 1.74 g/cm^3 for Mg and 2.62 g/cm^3 for MgB_2 . The crystal structure of MgB_2 composite material was analyzed by the $\text{Cu K}\alpha$ x-ray diffraction measurements. Resistivity and specific heat measurements were carried out in the range from 2 to 300 K using the physical property measurement system (PPMS, Quantum Design Co. Inc.). Magnetization data were accumulated by a SQUID magnetometer (MPMS, Quantum Design Co. Inc.) in the same temperature range.

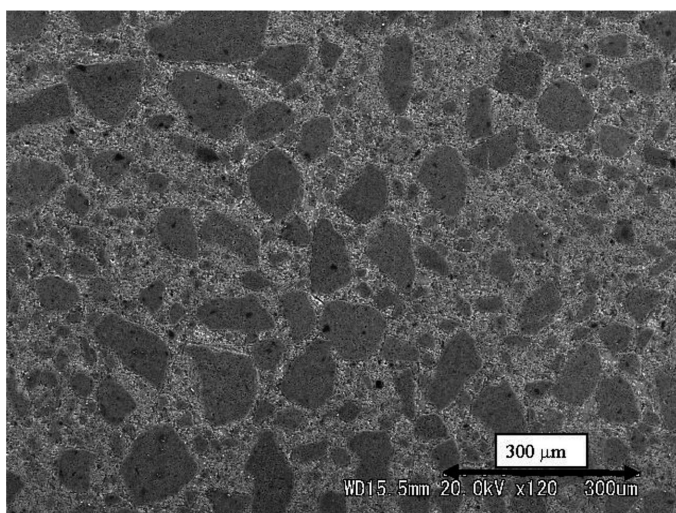


Fig. 1. SEM image at a cut surface of the $\text{MgB}_2/\text{Mg-9wt\%Zn}$ composite sample

3. Results and discussion

Figure 2 shows XRD patterns of the present samples together with the previous data of $\text{MgB}_2/\text{Mg-9wt\%Al-1wt\%Zn}$ [21] for a comparison. The peaks of MgB_2 -phase (marked with open circle) and Mg (closed circle) were observed. There are unknown peaks near 36 and 40 degrees with the AZ91 sample. In our previous paper [21] we speculated them as peaks from Mg-Zn alloys and ZnO referring other literature [9, 22]. A detailed investigation, however, indicated that the peaks are likely due to the $\text{Mg}_{17}\text{Al}_{12}$ precipitation. Doping Zn to Mg-Al alloys reduced the solid solubility of Al in Mg, resulting in precipitation of $\text{Mg}_{17}\text{Al}_{12}$ [23]. The lattice parameters of MgB_2 were found to change little with Zn contents, e.g. $a = 0.3091 \text{ nm}$ and $c = 0.3532 \text{ nm}$ with Z1 sample and $a = 0.3089 \text{ nm}$ and $c = 0.3528 \text{ nm}$ with Z6 sample.

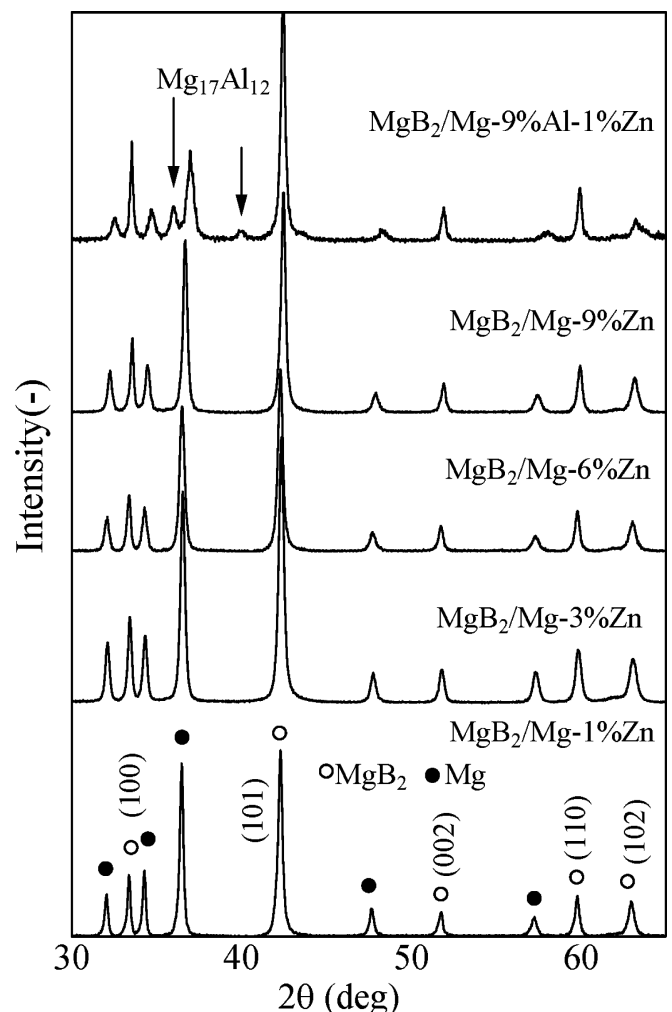


Fig. 2. The x-ray powder diffraction pattern of MgB_2 with Mg-Zn and $\text{Mg-9wt\%Al-1wt\%Zn}$ [21]

Low temperature parts of the electrical resistivity data were shown in Fig. 3. The T_c value estimated as an average of T_c (on set) and T_c (off set) and the residual resistivity (ρ_0) as an average of those around 40 K are listed in Table 1, in which the results of M0 and AZ91 samples are quoted from the previous work [21]. Comparing the present results of T_c and ρ_0 with those of $\text{MgB}_2/\text{Mg-Al-Zn}$ system, the T_c and ρ_0 variations with Z1 – Z9 samples are surprisingly small;

i.e. the doped Al element brought about a significant effect on the electron conductivity. The substitution of Al for Mg in MgB_2 has been considered to fill the electronic state and decrease the density of state at the Fermi level, leading to the decrease of T_c [24]. Although, in the SS-3DPC process, the MgB_2 particles were seen to keep their shape, doped Al most likely diffused into the MgB_2 particles and partly substituted Mg sites and made precipitations, which disturbed electron conductivity and coherence of electron pairs.

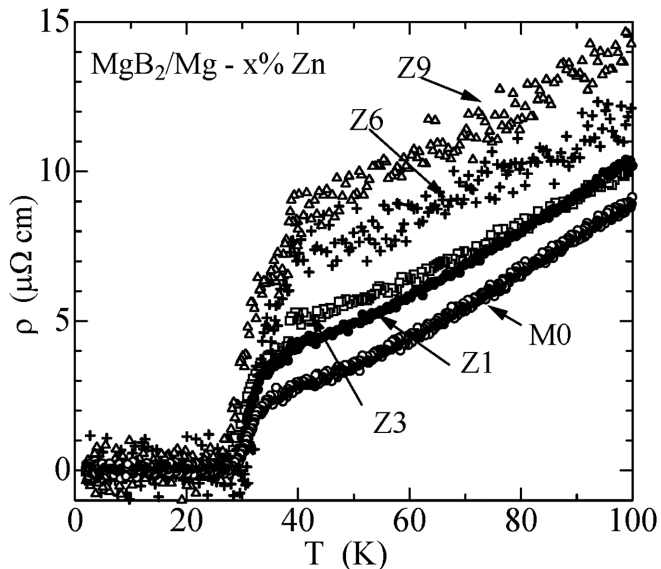


Fig. 3. Temperature dependence of resistivity of $\text{MgB}_2/\text{Mg} - x\% \text{ Zn}$ ($x = 0 - 9$, below 100 K)

TABLE 1

Host material, abbreviate letter for the sample, critical temperature estimated from ρ , residual resistivity ρ_0 around 40 K, upper critical field estimated from $\rho(T, H)$, superconducting volume fraction at 5 K, lower critical field at 5 K, critical current density at 1 T and 5 K

host material	label	T_c K	ρ_0 $\mu\Omega\text{cm}$	$H_{c2}(0)$ T	vol. %	H_{c1} mT	J_c kA/cm ²
Mg*	M0	33.7	2.9	—	65	50	5.3
Mg+1%Zn	Z1	33.1	4.2	5.2	48	37	3.8
Mg+3%Zn	Z3	32.5	5.2	4.4	46	42	5.2
Mg+6%Zn	Z6	34.6	7.6	6.8	53	48	4.8
Mg+9%Zn	Z9	33.2	8.6	5.2	54	47	5.6
Mg+9%Al+1%Zn*	AZ91	26.4	36.9	—	56	54	15.8

* These results were quoted and estimated from the data in ref. [21]

The temperature dependence of resistivity at several externally applied fields was measured for the Z1 – Z9 samples. The normalized resistivity $\rho(T, H)/\rho_0$ using the ρ_0 values listed in Table 1 for Z1 sample is shown in Fig. 4. The upper critical field H_{c2} was determined from the offset points of the transition temperature in the $\rho(T, H)/\rho_0$ curve. The temperature dependence of $H_{c2}(T)$ are shown in Fig. 5, which indicates that H_{c2} varies almost linearly with T . Extrapolation to $T = 0$ K with a linear fit of the data points for each sample results in the values of $H_{c2}(0)$ in Table 1. The deduced $H_{c2}(0)$ values are

a little related with the observed T_c values, but rather smaller than the reported values for bulk MgB_2 samples: e.g. for a single crystal with field along the c-plane, $H_{c2}(0) = 14.5$ T and field along the c-axis, $H_{c2}(0) = 3.2$ T [25].

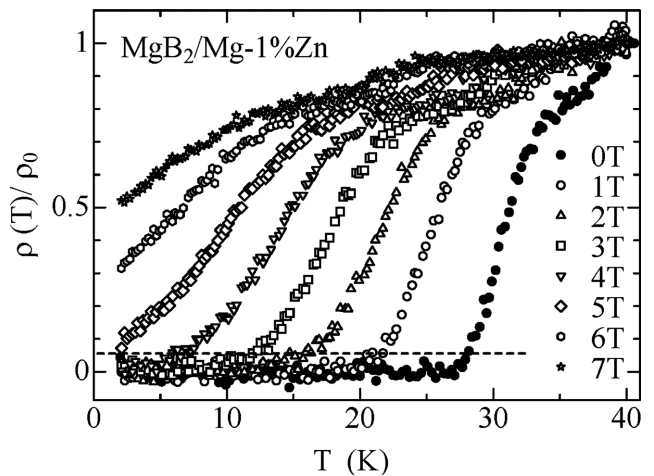


Fig. 4. Temperature dependence of normalized electrical resistivity $\rho(T, H)/\rho_0$ under several external fields for $\text{MgB}_2/\text{Mg} - 1\% \text{ Zn}$

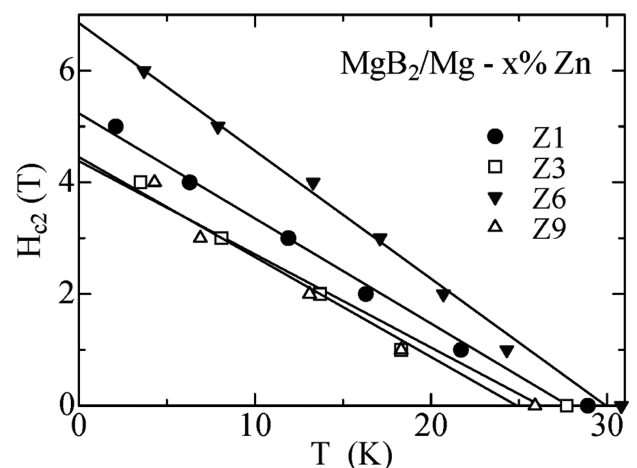


Fig. 5. Temperature dependence of upper critical field for $\text{MgB}_2/\text{Mg} - x\% \text{ Zn}$

The hysteresis loops of magnetizations are shown in Fig. 6. There is little obvious change in magnitude of the magnetization with doping Zn element. (The data points with M0 and Z1 – Z9 almost overlapped each other, but those of AZ91 are apparently larger than the others) The volume fractions of the superconducting part of the samples and the lower critical field H_{c1} at 5 K were estimated from the initial $M-H$ data points below 0.2 T. A H_{c1} value for certain x was taken as the field at which $M(H)$ curve deviates from the linear relation expected for the perfect diamagnetism, and the slope value provides the volume fraction, which is almost the same as the nominal value of MgB_2 powder against the host material. This result implies that the host materials banded MgB_2 particles without melting them. The $M-H$ loop curves also imply that doping Zn element did not enhance J_c since J_c linearly depends on the amplitude of the magnetization difference at a given field. The critical current density $J_c(H)$ of the samples (listed in Table 1) were evaluated using the equation of an extended Bean critical state model [26, 27] of

$J_c(H) = 20\Delta M / a(1 - a/3b)$, where ΔM is the amplitude of the M - H curve in emu/cm^3 at given field and temperature, and a and b are the sample length and width, respectively. This result quite contrasts to that of $\text{MgB}_2/\text{Mg-Al-Zn}$ system, in which the simultaneously doped Al and Zn elements increased J_c . This fact suggests that the J_c enhancement observed in $\text{MgB}_2/\text{Mg-Al-Zn}$ system is predominantly ascribed to substitution of Al for Mg and precipitation of $\text{Mg}_{17}\text{Al}_{12}$ (observed x-ray diffraction) stimulated by Zn addition.

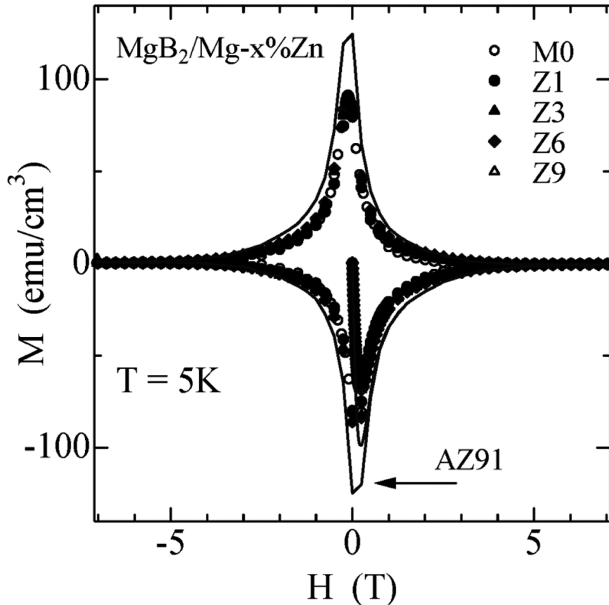


Fig. 6. M - H hysteresis loops for $\text{MgB}_2/\text{Mg} - x\%$ Zn at 5 K

Resistivity and magnetization often give misleading information on the bulk superconducting property. Resistivity is sensitive to the first percolation path, but no information can be extracted below T_c . Magnetization is sensitive to shielding by a superconducting superficial layer, so a precise calculation of the demagnetization factor is required to estimate a superconducting volume fraction. Specific heat measurements, in contrast, provide information on the bulk property. The specific heat jump is directly proportional to the superconducting volume, and its shape mirrors the distribution of T_c . Figure 7 presents an experimental result of specific heat measurement for the Z6 sample of 22.26 mg.

The measurements were carried out without field (data points were marked by closed circle) and then, with a field of 7 T (open circle) in Fig. 7(a) by the C/T versus T^2 scale. The specific heat jump due to the superconducting phase transition is noticeable. We estimate the specific heat difference between the superconducting and normal states ($\Delta C = C(0\text{T}) - C(7\text{T})$) as shown in Fig. 7(b). The $\Delta C/T$ variation against temperature surprisingly resembles to those in literature for pure MgB_2 [28, 29]. The calculated $\Delta C/T_c$ value in Fig. 7(b) is 0.035mJ/g K^2 , which is about 55 % of a typical reported one of $3.0\text{mJ/mol K}^2 (= 0.065\text{mJ/g K}^2)$ for pure MgB_2 [29]. This value of the superconducting volume fraction is almost the same as that obtained from the M - H data (see Table 1), supporting our data analysis with M - H data. The observed broad peak of $\Delta C/T$ has been associated with the two-band gap for MgB_2 electronic structure [28]. The specific heat curves in superconducting and normal states intersect at the temperature of $0.52T_c$ for a

weak-coupling superconductor [30]; this is definitely observed in the present sample.

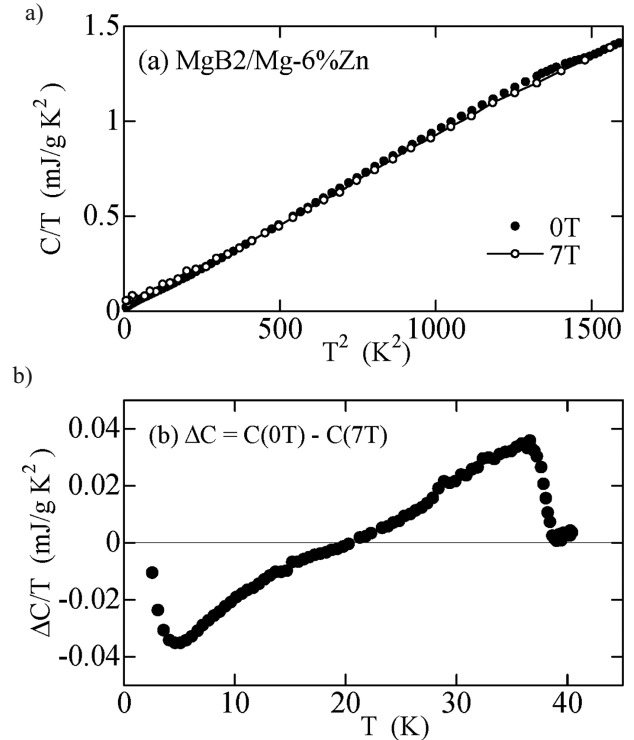


Fig. 7. (a) Specific heat of $\text{MgB}_2/\text{Mg-6\%Zn}$ sample with zero field (closed circle) and a field of 7 T (open circle) in C/T - T^2 scale. (b) The specific heat difference between the superconducting $C(0\text{T})$ and normal $C(7\text{T})$ states estimated from the data (a)

4. Conclusion

The present experimental work demonstrates that the three-dimensional penetration method combined with semi-solid casting is a suitable process to fabricate MgB_2 powder-magnesium-zinc alloys composite materials. The observed superconducting properties, such T_c , J_c , and ΔC , are comparable to those of pure MgB_2 bulk sample. Doping Zn element to MgB_2/Mg composites little enhanced J_c , being different from the results observed in $\text{MgB}_2/\text{Mg-Al-Zn}$ system. The present results confirm that doped Al to MgB_2/Mg composite raised a predominant effect on the J_c enhancement due to substitution for Mg, and doped Zn brought about an additional effect on the J_c enhancement by stimulating precipitation of $\text{Mg}_{17}\text{Al}_{12}$ which could work as a pinning center.

Acknowledgements

This study was partially supported by the Japan Society for the Promotion of Science (No. 22360313).

REFERENCES

- [1] J. Nagamatsu, N. Nakagawa, T. Muranaka, Y. Zenitani, J. Akimistu, Nature **410**, 63 (2001).
- [2] V. Braccini et al. Phys. Rev. **B71**, 012504 (2005).

- [3] T. Masui, S. Lee, A. Yamamoto, S. Tajima, *Physica C* **378-381**, 216 (2002).
- [4] T. Klein, L. Lyard, J. Marcus, Z. Holanová, C. Marcenat, *Phys. Rev.* **B73**, 184513 (2006).
- [5] K. Tanaka, M. Okada, M. Hirakawa, H. Yamada, H. Kumakura, H. Kitaguchi, *Supercond. Sci. Technol.* **18**, 678 (2005).
- [6] K. Tanaka, K. Funaki, T. Sueyoshi, Y. Sasashige, K. Kajikawa, M. Okada, H. Kumakura, H. Hayashi, *Supercond. Sci. Technol.* **21**, 095007 (2008).
- [7] E.W. Collings, M.D. Sumption, M. Bhatia, M.A. Susner, S.D. Bohnenstiehl, *Supercond. Sci. Technol.* **2**, 1030011 (2008).
- [8] W.K. Yeoh, S.X. Dou, *Physica C* **456**, 170 (2007).
- [9] P. Toulemonde, N. Musolino, H.L. Suo, R. Flukiger, *J. Supercond.* **15**, 613 (2002).
- [10] P. Toulemonde, N. Musolino, R. Flukiger, *Supercond. Sci. Technol.* **16**, 231 (2003).
- [11] S. Soltanian, X.L. Wang, J. Horvat, S.X. Dou, M.D. Sumption, M. Bhatia, E.W. Collings, P. Munroe, M. Tomsic, *Supercond. Sci. Technol.* **18**, 658 (2005).
- [12] P.P. Singh, P.J.T. Joseph, *J. Phys. Condens. Matter* **14**, 12441 (2002).
- [13] P.P. Singh, *Bull. Matter. Sci.* **26**, 131 (2003).
- [14] P.P. Singh, *Solid State Comm.* **127**, 271 (2003).
- [15] J.M. Rowell, *Supercond. Sci. Technol.* **16**, R17 (2003).
- [16] A. Yamamoto, J. Shimoyama, K. Kishio, T. Matsushita, *Supercond. Sci. Technol.* **20**, 658 (2007).
- [17] T. Matsushita, M. Kiuchi, A. Yamamoto, J. Shimoyama, K. Kishio, *Supercond. Sci. Technol.* **21**, 015008 (2008).
- [18] K. Matsuda, T. Saeki, K. Nishimura, S. Ikeno, Y. Yabumoto, K. Mori, *Materials Transactions* **47**, 1214 (2006).
- [19] S.X. Dou, X.L. Wang, J. Horvat, D. Milliken, A.H. Li, K. Konstantinov, E.W. Collings, M.D. Sumption, H.K. Liu, *Physica C* **361**, 79 (2001).
- [20] K. Matsuda, K. Nishimura, S. Ikeno, K. Mori, S. Aoyama, Y. Yabumoto, Y. Hishinuma, I. Mullerova, L. Frank, V.V. Yurchenko, T.H. Johansen, *J. Phys. Conf. Series* **97**, 012230 (2008).
- [21] Y. Shimizu, K. Matsuda, M. Mizutani, K. Nishimura, T. Kawabata, S. Ikeno, Y. Hishinuma, S. Aoyama, *Materials Transactions* **52**, 272 (2011).
- [22] Y. Kimishima, Y. Sugiyama, S. Numa, M. Uehara, T. Kuramoto, *Physica C* **468**, 1185-1187 (2008).
- [23] S. Celotto, *Acta mater.* **48**, 1775 (2000).
- [24] J.S. Slusky, N. Rogado, K.A. Regan, M.A. Hayward, P. Khalifah, T. He, K. Inumaru, S.M. Loureiro, M.K. Haas, H.W. Zandbergen, R.J. Cava, *Nature* **410**, 343-345 (2001).
- [25] M. Zehetmayer, M. Eisterer, J. Jun, S.M. Kazakov, J. Karpinski, A. Wisniewski, H.W. Weber, *Phys. Rev.* **B66**, 052505 (2002).
- [26] C.P. Bean, *Phys. Rev. Lett.* **8**, 250 (1962).
- [27] Z. Cheng, B. Shen, J. Zhang, S. Zhang, T. Zhao, H. Zhao, *J. Appl. Phys.* **91**, 7125 (2002).
- [28] H.J. Choi, D. Roundy, H. Sun, M.L. Cohen, S.G. Louie, *Nature* **418**, 758-760 (2002).
- [29] H.D. Yang, J.-Y. Lin, H.H. Li, F.H. Hsu, C.J. Liu, S.-C. Li, R.-C. Yu, C.-Q. Jin, *Phys. Rev. Lett.* **87**, 167003 (2001).
- [30] Y. Wang, T. Plackowski, A. Junod, *Physica C* **355**, 179 (2001).